Biosensors and Bioelectronics 26 (2010) 536–541

Contents lists available at ScienceDirect

Biosensors and Bioelectronics

journal homepage: www.elsevier.com/locate/bios

Reagentless biosensor for hydrogen peroxide based on self-assembled films of horseradish peroxidase/laponite/chitosan and the primary investigation on the inhibitory effect by sulfide

Dan Shan[a,*], Qing-Bo Li[a], Shou-Nian Ding[b], Jia-Qi Xu[a], Serge Cosnier[c], Huai-Guo Xue[a]

[a] Key Laboratory of Environmental Material & Environmental Engineering of Jiangsu Province, School of Chemistry & Chemical Engineering, Yangzhou University, Si Wangting Road 180, Yangzhou, Jiangsu 225002, China
[b] School of Chemistry & Chemical Engineering, Southeast University, Nanjing 211189, China
[c] Département de Chimie Moléculaire UMR-5250, ICMG FR-2607, CNRS Université Joseph Fourier, BP-53, 38041 Grenoble, France

ARTICLE INFO

Article history:
Received 17 January 2010
Received in revised form 13 July 2010
Accepted 14 July 2010
Available online 22 July 2010

Keywords:
Direct electron transfer
Self-assembly
Laponite
Horseradish peroxidase
Sulfide

ABSTRACT

Horseradish peroxidase (HRP) was successfully incorporated into the laponite/chitosan (Chit)-modified glassy carbon electrode (GCE) using step-by-step self-assembly. The self-assembly processes were monitored by X-ray photoelectron spectroscopy (XPS) and electrochemical impedance spectra (EIS). Direct electrochemistry and electrocatalysis of the self-assembled HRP were investigated. Cyclic voltammetry of HRP/laponite/Chit/GCE, in anaerobic phosphate buffer solution (0.025 M PBS, pH 7.0), displayed a pair of stable and quasi-reversible peaks at potentials E_{pa} = 0.024 V and E_{pc} = −0.132 V vs. SCE, attributed to the HRP-Fe(III)/HRP-Fe(II) redox couple. The electrochemical reaction of the HRP/laponite/Chit/GCE exhibited a surface-controlled electrode process. The electron transfer rate constant was estimated to be 1.82 s^{-1}. The self-assembled HRP maintained its biological activity and exhibited an excellent electrocatalytic performance for the reduction of H_2O_2 with fast amperometric response (10 s), broad linear range (2.9×10^{-5} to 1.4×10^{-3} M), good sensitivity (19.7 ± 0.5 mA M^{-1} cm^{-2}) and low detection limit (5×10^{-6} M) at a signal-to-noise ratio of 3. Moreover, the inhibitory of sulfide to the self-assembled HRP was also investigated.

1. Introduction

Sulfides (H_2S, HS^- and S^{2-}) can be found widely in natural water samples and wastewater. The long-term action of sulfide in low concentrations causes chronic diseases of respiratory tracts, blood, eyes, skin and digestive disturbance. Thus, the high toxicity of sulfide species and reactivity of sulfide species have made their measurement crucial to both analytical and environmental chemists (Titova et al., 2009). A variety of analytical methods for determining sulfides have been reported to data. These methods include spectrophotometric (Kosyakov et al., 2010; Čmelik et al., 2010), chemiluminescence (Safavi and Karimi, 2002), UV-spectrophotometric (Guenther et al., 2001), ion-chromatographic (Kolotilina and Dolgonosov, 2005).

The electrochemical techniques are particularly attractive as they often provide sensitive, unpretentious design, low cost and fast-responsive detection methods (Lawrence et al., 2000). Yang et al. have demonstrated the feasibility of quantitatively detecting sulfides through their inhibition effect on an enzyme electrode based on HRP immobilized on a cysteamine self-assembled monolayer (Yang et al., 2004). The inhibitive measurement of sulfides was performed in the presence of an electron mediator hydroquinone in 0.067 M PBS (pH 6.5) at an applied potential of −150 mV vs. SCE (Yang et al., 2004). Nevertheless, the addition of mediator into the test solution brings more application limitation.

In the present work, we constructed a novel sulfide determination system based on its inhibitory effect on a reagentless biosensor for hydrogen peroxide. The direct electron transfer between HRP molecule and electrode is very difficult to achieve because of the deeply buried electro-active centers in HRP. Direct electron transfer of protein depends strongly on the immobilization procedure, the nature of the support, and the properties and the stability of the biomolecule (Freire et al., 2003; Shan et al., 2009a). The self-assembly owns unprecedented flexibility to tailor interfacial properties and presents biologically relevant groups, which makes it well-suited for control of biomolecular density and orientation at the solid–liquid interface to obtain better reproducibility and higher efficiency (Shan et al., 2007). Following our previous protocol (Shan et al., 2007), herein HRP was incorporated on laponite/Chit film based on stepwise self-assembly technique.

Chit is a copolymer of glucosamine and N-acetylglucosamine units; it is a product of partial chitin deacetylation and may

* Corresponding author. Fax: +86 514 87975244.
E-mail address: danshan@yzu.edu.cn (D. Shan).

0956-5663/$ – see front matter © 2010 Elsevier B.V. All rights reserved.
doi:10.1016/j.bios.2010.07.051

contain N-acetylated groups. It displays a rare combination of physicochemical properties that include the excellent film-forming ability, high permeability toward water, good adhesion, and biocompatibility (Krajewska, 2004, 2005). Moreover, its amino group could react with –COOH through dehydration reaction and covalent assembly on the functional electrode surface (Zhao et al., 2005). Laponite is a synthesized hectorite with the formula of $(Mg_{5.5}Li_{0.5})Si_4O_{10}(OH)_2(Na^+_{0.73}{\cdot}nH_2O)$ (Tanabe et al., 1989). It is significantly smaller than naturally occurring clay. Thanks to the distinguished interfacial properties, this attractive material has been successfully used to construct the biosensors (Shi et al., 2008; Fan et al., 2007; Shan et al., 2002, 2003; Mousty et al., 2001) and realize the direct electrochemistry of the enzymes such as xanthine oxidase (Shan et al., 2009a), glucose oxidase (Shan et al., 2009b) and hemoglobin (Shan et al., 2007). Chit is positively charged in aqueous acidic media (pH < 6.5), negatively charged laponite can be anchored on the Chit-modified electrode via electrostatic attraction. The isoelectric point of HRP was reported at pH 8.9 (Zhou et al., 2002); at pH 6.0, the enzyme is positively charged. Therefore, the final incorporation of HRP into laponite/Chit film modified electrode can be readily achieved. The self-assembly of the stepwise courses was monitored by XPS and EIS.

2. Experimental

2.1. Materials

Horseradish peroxidase (HRP) (EC 1.11.1.7, type II, 140 U mg^{-1}) was purchased from Amresco. Chitosan (Chit, MW $\sim 1 \times 10^6$; >90% deacetylation) was obtained from Shanghai Reagent Company (China). Laponite (monovalent cation exchange capacity: CEC = 0.74 mmol g^{-1}) was obtained from Rockwood Specialities Inc (Princeton, NJ). All other chemicals were of analytical grade and used without further purification. H_2O_2 was freshly prepared before being used. Phosphate buffer solution (PBS) was 0.025 M K_2HPO_4 and KH_2PO_4 and its pH was adjusted with H_3PO_4 or KOH solutions. Twice-distilled water was used through out the experiment.

2.2. Measurements and apparatus

A CHI 660 electrochemical workstation (CH Instruments) was used for cyclic and amperometric voltammetry. A three-electrode cell was used with a saturated calomel electrode (SCE) as reference electrode, a platinum wire as counter electrode, and the modified GCE (diameter 3 mm) as working electrode on which HRP/laponite/Chit film was successively immobilized. Electrolytic solutions were purged with highly purified nitrogen for at least 20 min prior to the series of experiments. A nitrogen environment was then kept over solution in the cell to prevent the contact of the solution from oxygen. X-ray photoelectron spectroscopy (XPS) measurements were performed on ESCALab220I-XL spectrometer with Al Ka X-ray radiation as the X-ray source for excitation and analyzer pass energy of 20 eV. Electrochemical impedance spectra (EIS) measurements were conducted using an Autolab/PGSTAT30 with a three-electrode system. The EIS measurements were performed in 5 mM $Fe[(CN)_6]^{3-/4-}$ containing 0.1 M KCl. The amplitude of the applied sine wave potential was 5 mV. The impedance measurements were recorded at a bias potential of 180 mV within the frequency range of 0.05 –10 kHz.

2.3. Preparation of HRP/laponite/Chit/GCE

To obtain good cyclic voltammetric responses of HRP/laponite/Chit/GCE, the following conditions were optimized in control experiments. A 1.0-wt% Chit solution was prepared by dissolving Chit flakes in 0.5-wt‰ acetic acid (HAc). The laponite colloid suspension (0.5 mg ml^{-1}) was prepared by dispersing laponite in deionized water with stirring overnight. HRP was dissolved in 0.025 M PBS (pH 6.0) with a concentration of 2 mg ml^{-1}. Prior to use, a 3-mm-diameter glassy carbon electrode (GCE) was polished on a polishing cloth with alumina of successively smaller particles (1.0 μM diameter). Then the electrode was cleaned by ultrasonication in deionized water. After that, it was oxidized at 1.5 V for 5 min in the solution containing 10% HNO_3 and 2.5% $K_2Cr_2O_7$, by which –COOH could be formed on the surface of GCE. After washed with water, GCE was immersed into Chit solution for about 10 h at 50 °C. The resulting electrode was then dipped into laponite solutions for 10 h; finally, the laponite/Chit-modified GCE was incubated into HRP solution for about 12 h to attach proteins. The resultant electrode is denoted as HRP/laponite/Chit/GCE. All the protein electrodes were washed with water and stored in 0.025 M PBS (pH 7.0) at 4 °C when not in use.

2.4. Inhibitive measurement procedure

The HRP/laponite/Chit/GCE was dipped into a stirred 0.025 M PBS (pH 7.0) for 20–30 min until a stable baseline output signal was reached. Determine the initial current response (I_1) of the biosensor to H_2O_2 solution of a given concentration (i.e. 0.5 mM). Determine the current response (I_2) of the biosensor to the H_2O_2 solution of the same concentration in the presence of sulfide. The degree of inhibition (Inhibition %) is then calculated by making a comparison between the current responses before and after addition of inhibitor according to the equation generally used (Shan et al., 2004a,b):

$$\text{Inhibition}\,(\%) = \frac{I_1 - I_2}{I_1} \times 100$$

Each experiment was repeated at least three times and a relative standard deviation of the output signal was estimated to be not more than 5%. The control experiment for H_2O_2 without the inhibitor was performed after each inhibitor measurement.

3. Results and discussion

3.1. Characterization of the self-assembled HRP/laponite/Chit film

3.1.1. XPS measurements

XPS measurements were performed to obtain the elemental composition of the self-assembled films in the stepwise course in order to confirm the immobilization of each layer. Fig. 1 presents the XPS survey scans of the surface for the functional GCE (a), Chit/GCE (b), laponite/Chit/GCE (c), and HRP/laponite/Chit/GCE (d) in the range of 0–1000 eV. The functional GCE surface shows C_{1s} and O_{1s}, the latter is attributed to –COOH formed by the electrochemical oxidation of bare GCE in the solution containing 10% HNO_3 and 2.5% $K_2Cr_2O_7$ (Fig. 1a). The main elements of Chit/GCE surface are C, O and N (Fig. 1b). N_{1s} stems from the amino group of Chit. The observed elements Na and Mg in Fig. 1c are due to the electrostatic self-assembly of laponite on the Chit-modified GCE. The self-assembly of HRP in the laponite/Chit film can be further demonstrated by the element Fe in the XPS survey scan of the HRP/laponite/Chit/GCE (Fig. 1d).

3.1.2. Electrochemical impedance spectroscopy

EIS can provide useful information about the impedance changes of the electrode surface during the fabrication process (Fan et al., 2007). The Nyquist plot of the EIS includes a semicircular portion and a linear portion. The semicircular portion at higher frequencies corresponds to the electron-transfer-limited process and its diameter is equal to the electron transfer resistance (R_{CT}),

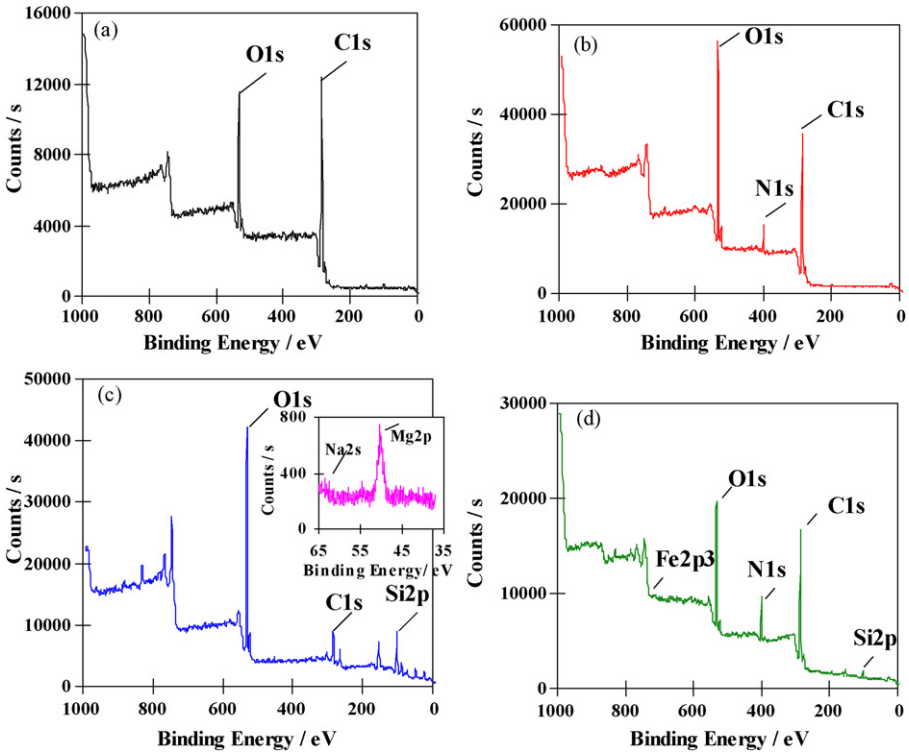

Fig. 1. The XPS complete spectroscopy of (a) the functional GCE, (b) Chit/GCE, (c) laponite/Chit/GCE, and (d) HRP/laponite/Chit/GCE.

which controls the electron-transfer kinetics of the redox probe at the electrode interface (Bard and Faulkner, 2001). Fig. 2 displays the Nyquist plots of the EIS of a bare GCE (a), Chit/GCE (b), laponite/Chit/GCE (c), and HRP/laponite/Chit/GCE (d) in 5.0 mM $K_3Fe(CN)_6/K_4Fe(CN)_6$ (1:1) containing 0.1 M KCl. Changes of the impedance spectra are observed in the course of stepwise modification of the electrode, and the R_{CT} values of the bare GCE, Chit/GCE, laponite/Chit/GCE, and HRP/laponite/Chit/GCE are ca. 241, 635, 1319 and 2011 Ω. The increased R_{CT} implies the increased interfacial resistance due to the self-assembled non-conductive molecules in the stepwise self-assembly. The dramatically increased R_{CT} in the last process of self-assembly indicates that the successful immobilization of HRP via self-assembly.

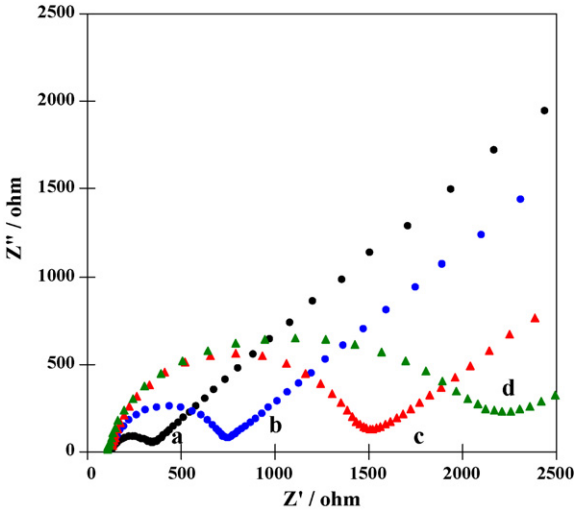

Fig. 2. Electrochemical impedance spectroscopy of bare GCE (a), Chit/GCE (b), laponite/Chit/GCE (c), and HRP/laponite/Chit/GCE (d) in 0.1 M KNO_3 solution containing 5.0 mM $Fe(CN)_6^{3-}/Fe(CN)_6^{4-}$ (1:1).

3.2. Direct electrochemistry of HRP/laponite/Chit-modified GCE

Fig. 3 shows the cyclic voltammogarms of the bare GCE (a) and the self-assembled HRP/laponite/Chit/GCE (b) in 0.025 M PBS (pH 7.0) under the anaerobic condition at a scan rate of 100 mV s^{-1}. A pair of well-defined redox peaks, which can be ascribed to the electron transfer between the self-assembled HRP and the underlying electrode, is observed at the HRP/laponite/Chit-modified GCE (curve *b* in Fig. 3). The anodic peak potential (E_{pa}) and cathodic peak potential (E_{pc}) are located at 0.024 and −0.132 V, respectively. Its formal potential (defined as the average of E_{pa} and E_{pc}), $E^{0'}$, is ca. −0.054 V (at 100 mV s^{-1}), which is positive than those obtained for native HRP in solution (Harbury, 1957), HRP at TiO_2 nanotube arrays (Wu et al., 2008), and Clay-HRP-Clay/AuCs-GCE (Zhao et al., 2008). This phenomenon may be ascribed to the electrostatic interaction between the positively charged HRP and the negatively charged laponite nanoparticles that strongly affect the heme microenvironment (Wu et al., 2008; Zhao et al., 2008). In addition, this redox signal is quite stable, the peak height and peak potential of the self-assembled HRP/laponite/Chit film have remained nearly unchanged, and the amount of degradation after 50 cycles in N_2-saturated PBS with a scan rate of 100 mV s^{-1} was less than 1%.

The effect of scan rate on the response of the self-assembled HRP is shown in Fig. 3B. Peak currents vary linearly with the scan rates in a range from 20 to 1200 mV s^{-1}, as shown in the Inset I of Fig. 3B. The linear regression equations are I_{pa} (μA) = 27.29ν (V s^{-1}) + 1.15, R^2 = 0.9987 (n = 10); I_{pc} (μA) = −27.33ν (V s^{-1}) − 1.07, R^2 = 0.9988 (n = 10), respectively. This suggests that the electron transfer process for the self-assembled HRP/laponite/Chit/GCE is a surface-confined mechanism in the potential scope mentioned above. According to the slope of the I_p–ν curve and the following equation $I_p = n^2F^2\nu A\Gamma/4RT$ (Laviron, 1979), where Γ is the average surface coverage of the electrode redox substance (mol cm^{-2}), and A the electrode area (0.07 cm^2), n, F, R and T have their same meaning. For this electrode, the Γ is estimated to be

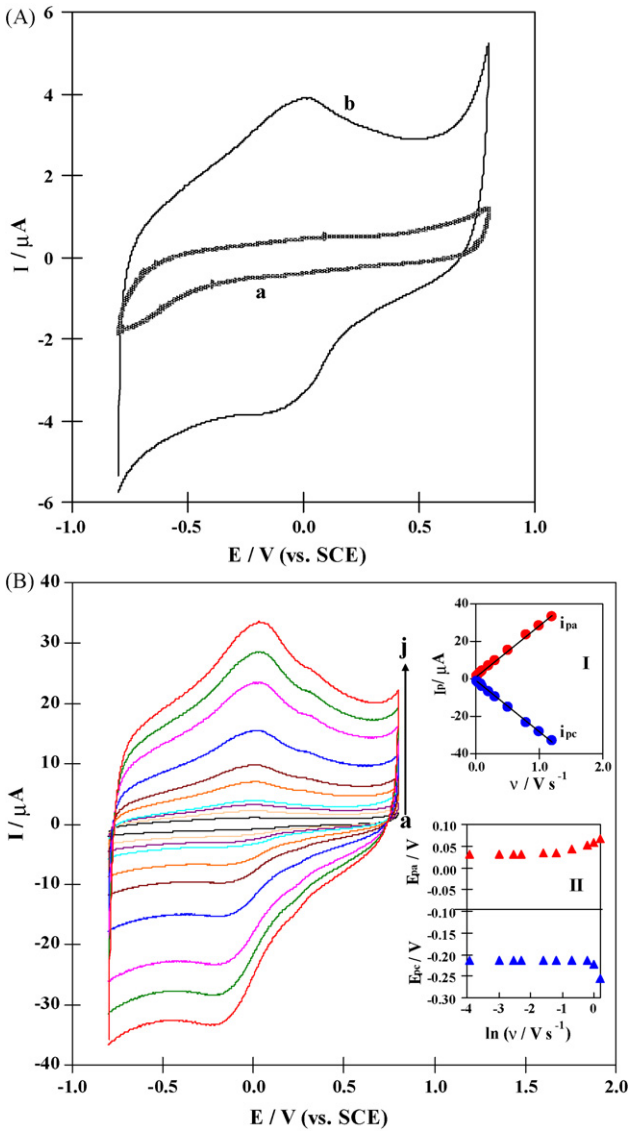

Fig. 3. (A) Cyclic voltammograms of bare GCE (a) and HRP/laponite/Chit/GCE (b) in 0.025 M PBS (pH 7.0) at a scan rate of 100 mV s^{-1}. (B) Cyclic voltammograms of the self-assembled HRP/laponite/Chit-modified GCE in 0.025 M PBS (pH 7.0) at various scan rates. The scan rate from inner to outer are (a) 20 mV s^{-1}, (b) 50 mV s^{-1}, (c) 80 mV s^{-1}, (d) 100 mV s^{-1}, (e) 200 mV s^{-1}, (f) 300 mV s^{-1}, (g) 500 mV s^{-1}, (h) 800 mV s^{-1}, (i) 1000 mV s^{-1}, and (j) 1200 mV s^{-1}. Inset I: The plot of anodic and cathodic peak currents vs. scan rates. Inset II: the relation between the peak potentials and logarithm of ν.

4.16×10^{-10} mol cm^{-2}, which is much larger than those obtained by HRP/CeO_2/Chit/GCE (7.06×10^{-11} mol cm^{-2}) (Xiao et al., 2009), HRP in titanate nanosheet (8.60×10^{-11} mol cm^{-2}) (Zhang et al., 2007), and HRP immobilized on a cationic gemini surfactant-polyvinyl alcohol composite film (1.49×10^{-10} mol cm^{-2}) (Liu et al., 2009). As the theoretical value of monolayer coverage of HRP is about 5.1×10^{-11} mol cm^{-2} (Yamazaki et al., 1978), the experimental value is much higher than the theoretical one. Thus multilayer of HRP must be assembled and participate in the electrode reaction. Inset II of Fig. 3B shows the relationship between the peak potential E_p and the natural logarithm of scan rate lnν for HRP/laponite/Chit/GCE in 0.1 M PBS (pH 7.0). Based on the data obtained from Inset II of Fig. 3B and according to Laviron equation (Laviron, 1979):

$$E_p = E^{0'} + \frac{RT}{\alpha nF} - \frac{RT}{\alpha nF} \ln \nu$$

where α is the cathodic electron transfer coefficient, n is the number of electron, R, T and F have their usual meanings ($R = 8.314$ J mol^{-1} K^{-1}, $T = 298$ K, $F = 96,493$ C mol^{-1}), and αn was calculated to be 0.385. Given $0.3 < \alpha < 0.7$ in general (Ma et al., 2000), it could be concluded that $n = 1$ and $\alpha = 0.385$. So, the redox reaction between HRP and GCE was a single electron transfer process. In order to calculate the value of apparent heterogeneous electron transfer rate constant (k_s), the following Laviron equation was used (Laviron, 1979):

$$\log k_s = \alpha \log(1-\alpha) + (1-\alpha)\log\alpha - \log\frac{RT}{nF\nu} - \frac{\alpha(1-\alpha)nF\Delta E_p}{2.3RT}$$

where α is the electron transfer coefficient, n is the number of electron ΔE_p is the separation of the redox peaks, ν is the scan rate, R, T and F have their usual meaning, k_s was calculated to be 1.82 s^{-1}. This value is comparative to that obtained at ZnO-GNPs-Nafion-HRP/GCE (1.94 s^{-1}) (Xiang et al., 2009), HRP-AuNPs-SF/GCE (1.84 s^{-1}) (Yin et al., 2009), and higher than that obtained at HRP/MB/WSGE (0.12 s^{-1}) (Lin et al., 2000) and HRP-Au-SPCE (0.75 ± 0.04 s^{-1}) (Xu et al., 2003). This implies further that the fast electron transfer between HRP and GCE has been achieved by the self-assembled system based on laponite/Chit.

It is well known that the redox reaction of HRP-heme undergoes a one-electron coupled with one-electron mechanism. Thus, the electrochemical behaviors of the self-assembled HRP/laponite/Chit/GCE should be pH dependent. In the range of pH (4.0–9.0), the HRP/laponite/Chit/GCE can exhibit a pair of stable and well-defined redox peaks. An increase of solution pH from pH 4.0 to 9.0 led to a negative shift of both oxidation and reduction peak potentials (Fig. 4A). The linear regression equation is $E^{0'} = -0.049$ pH + 0.2554 ($R^2 = 0.9934$) (Fig. 4B). The slope of −49 mV pH^{-1} is slight different from the theoretical value of −58.6 mV pH^{-1} expected for a one-proton accompanied with one-electron redox reaction process. It might be attributed to the special ion-exchange ability of laponite. Laponite can exchange cations, and protons as well (Shan et al., 2007). The number of charges at the clay surface varies with pH, and then resulted in the different amount of exchanged protons (Pecorari and Bianco, 1998).

3.3. Electrocatalysis of HRP/laponite/Chit/GCE to reduction of H_2O_2

The determination of hydrogen peroxide is of great importance in chemical, biological, clinical, food, and environmental fields. The electrocatalytic properties of the enzyme electrode towards H_2O_2 are shown in Fig. 5. When H_2O_2 was injected to blank PBS, the onset of H_2O_2 reduction occurred near −0.3 V and the cathodic peak at around −0.65 V were observed (curve *a–e* of Inset A). Nevertheless, no direct reduction of H_2O_2 was found at HRP-free film electrode (laponite/Chit/GCE) in the presence of H_2O_2 at the same potential range. Thus, the catalytic current stems from the electrocatalytic reduction process of H_2O_2 by the self-assembled HRP electrode. Furthermore, the cathodic current increased with the increasing H_2O_2 concentration. These results further confirm that HRP self-assembled in the HRP/laponite/Chit film had good bioelectrocatalytic activity towards H_2O_2.

According to previous reports (Ghamouss et al., 2006; Yin et al., 2009), the mechanism of electrocatalytic reduction of H_2O_2 in this work can be expressed as follows:

$$HRP(Fe^{III}) + H_2O_2 \rightarrow \text{Compound I}(Fe^{IV} = O,\ P^{\bullet+}) + H_2O \quad (1)$$

$$\text{Compound I}(Fe^{IV} = O,\ P^{\bullet+}) + H_2O_2 \rightarrow HRP(Fe^{III}) + O_2 \quad (2)$$

$$HRP(Fe^{III}) + e^- \rightarrow HRP(Fe^{II})\,(\text{at electrode}) \quad (3)$$

$$HRP(Fe^{II}) + O_2 \rightarrow HRP(Fe^{II}\text{–}O_2)\,(\text{fast}) \quad (4)$$

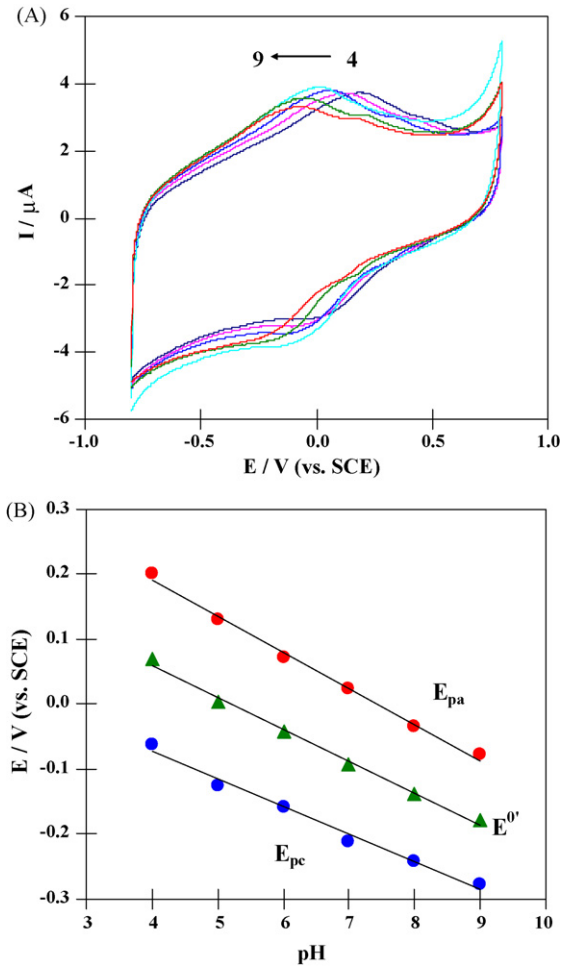

Fig. 4. (A) Cyclic voltammograms of the self-assembled HRP/laponite/Chit/GCE in 0.025 M PBS at 25 °C with different pH values of 4, 5, 6, 7, 8 and 9. Scan rate: 100 mV s^{-1}. (B) The effect of pH on E_{pa}, E_{pc} and the formal potential of the self-assembled HRP/laponite/Chit/GCE in 0.025 M PBS at 25 °C. Scan rate: 100 mV s^{-1}.

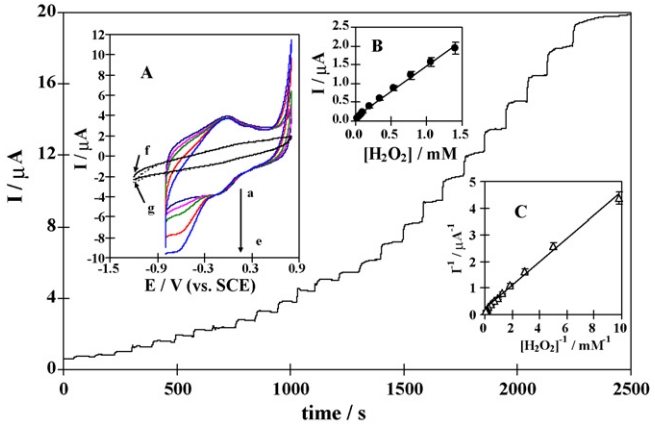

Fig. 5. Typical steady-state response of the self-assembled HRP/laponite/Chit/GCE on successive injection of H_2O_2 into 10 ml of stirring 0.025 M PBS (pH 7.0). Applied potential: −0.45 V vs. SCE. Inset A: Cyclic voltammograms of (a) HRP/laponite/Chit/GCE in 0.025 M PBS (pH 7.0) containing no H_2O_2; (b) HRP/laponite/Chit/GCE in 0.025 M PBS (pH 7.0) containing 0.3 mM H_2O_2; (c) HRP/laponite/Chit/GCE in 0.025 M PBS (pH 7.0) containing 0.75 mM H_2O_2; (d) HRP/laponite/Chit/GCE in 0.025 M PBS (pH 7.0) containing 1.75 mM H_2O_2; (e) HRP/laponite/Chit/GCE in 0.025 M PBS (pH 7.0) containing 2.5 mM H_2O_2; (f) laponite/Chit/GCE in 0.025 M PBS (pH 7.0) containing no H_2O_2 and (g) laponite/Chit/GCE in 0.025 M PBS (pH 7.0) containing 2.5 mM H_2O_2; scan rate: 100 mV s^{-1}. Inset B: the linear plot of calibration curve of the proposed electrode to H_2O_2. Inset C: linear curve of I^{-1} vs. $[H_2O_2]^{-1}$.

$$HRP(Fe^{II}–O_2) + 2e^- + 2H^+ \rightarrow HRP(Fe^{II}) + H_2O_2\,(\text{at electrode}) \quad (5)$$

In Eqs. (1) and (2), H_2O_2 acts as an oxidant and reductant, respectively, in which, HRP(Fe^{III}) is oxidized by H_2O_2 to produce an intermediate of compound I(Fe^{IV} = O, $P^{\bullet+}$) firstly, then Compound I is reduced by H_2O_2 through at a two-electron transfer pathway and produce native HRP(Fe^{III}) again and O_2. After HRP(Fe^{III}) accepting one electron from electrode to form HRP(Fe^{II}) shown as Eq. (3), HRP(Fe^{II}) reacts with O_2 in solution very rapidly to from HRP(Fe^{II}–O_2), which then undergoes electrochemical reduction at the electrode at the same potential as that of HRP(Fe^{III}) reduction, producing H_2O_2 and HRP-Fe(II) again and forming a catalytic cycle with Eq. (4). H_2O_2 produced in Eq. (5) will participate in Eq. (1) or (2) to produce O_2 which will then induce or promote the catalytic cycle of Eqs. (4) and (5).

The electrocatalytic reduction of hydrogen peroxide at HRP/laponite/Chit/GCE was also studied by amperometry, which is one of the most widely employed techniques for biosensor. Background current increased as the potential became more significant from −0.45 to −0.65 V. In addition, an optimum ratio of response-to-background current was observed at −0.45 V. Therefore, the amperometric measurement of the self-assembled HRP/laponite/Chit/GCE to H_2O_2 at an applied potential of −0.45 V upon successive addition of H_2O_2 into stirring 0.025 M PBS (pH 7.0) was performed (Fig. 5). Upon the addition of an aliquot of H_2O_2 to the buffer solution, the reduction current increases steeply to reach a stable value. The proposed self-assembled electrode achieves 95% of the steady-state current within 10 s. The response to H_2O_2 is linear in the range from 2.9×10^{-5} to 1.4×10^{-3} M, and with a linear regression equation for i (μA) = 1.34 [H_2O_2] (mM) + 0.091, R^2 = 0.9949 (n = 10) (Inset B of Fig. 5). The relative standard deviation (RDS) is 1.8% for n = 10. The linear range is wider than that obtained based on the direct electrochemical behavior of HRP immobilized on a gelatin-hydrophobic ionic liquid gel films (Yan et al., 2007) and that based on immobilized in a zirconia enhanced grafted collagen trihelix scaffold (Zong et al., 2006). The sensitivity was calculated to be 19.7 ± 0.5 mA M^{-1} cm^{-2}. A low detection limit of 5×10^{-6} M was determined at a signal-to-noise ratio of 3, which is lower than that of 12.89 μM of HRP immobilized in sol–gel-derived ceramic–carbon nanotube nanocomposite film (Chen and Dong, 2007) and 9.0 μM of HRP based on clay–chitosan–gold nanoparticle nanocomposite (Zhao et al., 2008).

The apparent Michaelis–Menten constant, which gives an indication of the enzyme-substrate kinetics, could be obtained from the electrochemical version of the Lineweaver–Burk equation (Kamin and Willson, 1980):

$$\frac{1}{I_{ss}} = \frac{1}{I_{max}} + \frac{K_M^{app}}{I_{max}C}$$

where I_{ss} is the catalytic current, C is the bulk concentration of the substrate, I_{max} is the maximum catalytic current under saturated substrate conditions, and K_M^{app} is the apparent Michaelis constant. K_M^{app} value for HRP/laponite/Chit film self-assembled modified GCE was found to be 2.14 mM, based on the slope and the intercept of the $1/I_{ss}$ versus $1/C$ plot (Inset C of Fig. 5).

3.4. Inhibitory effect of sulfide

Sulfides as inhibitor to HRP have long been established (Zhao et al., 1996; Yang et al., 2004). Thus, for the further comprehensive studies the biocatalytic behavior of the self-assembled HRP/laponite/Chit/GCE, we evaluated the inhibitory effect of sulfide. Upon the addition of sulfide to the test solution containing H_2O_2, the catalytic current decreased dramatically (curve c in Fig. 6). This phenomenon is indicative of the effective inhibitory of the immobilized HRP by NaS_2. However, the mechanism for

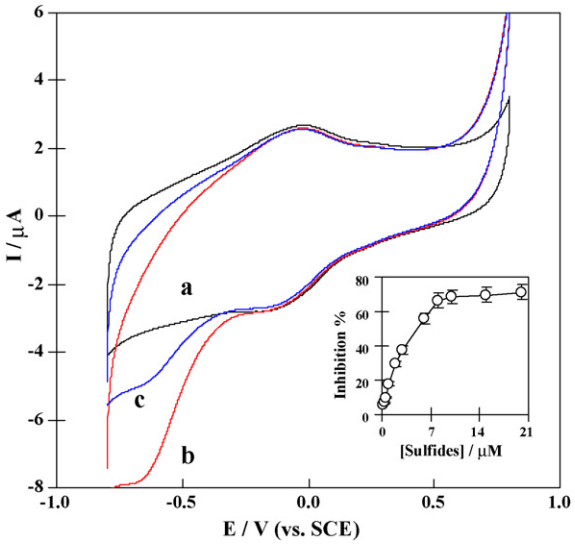

Fig. 6. Cyclic voltammograms of the self-assembled HRP/laponite/CHT/GCE at different stages: (a) the electrode in 0.025 M PBS (pH 7.0); (b) the same as (a) containing 2.5 mM H_2O_2; (c) the same as (b) with 25 μM Na_2S added; scan rate: 100 mV s^{-1}. Inset: inhibition calibration curve for sulfides determination with the proposed biosensor, the concentration H_2O_2 fixed as 0.5 mM.

this inhibition is not yet fully understood. As suggested by Zhao et al., sulfides were able to directly attack the heme group, causing much more severe inactivation by blocking the active site of HRP, and therefore inhibiting the reduced current of H_2O_2 (Zhao et al., 1996). Thus, the self-assembled HRP/laponite/Chit/GCE can be used to monitor the trace of sulfides via inhibition.

A typical inhibition calibration curve for the determination of sulfide is shown in inset of Fig. 6. HRP inhibition increased significantly with the addition of sulfide. The linear range is 0.2–8 μM with a slope of 7.801 (% μM^{-1}) and a correlation coefficient of 0.978 ($n = 8$). A maximum inhibition of about 70.4% was obtained for 20 μM sulfide. IC_{50}, i.e. the concentration of the inhibitor corresponding to 50% of the inhibition signal was calculated to be 5.3 μM from the data of inset of Fig. 6.

4. Conclusion

The immobilization of HRP can be readily achieved by step-by-step electrostatic self-assembly based on Chit and laponite nanoparticles. Chit and laponite serve as the important roles of "scaffold" in the architecture of the proposed electrode. In this configuration, the electrostatic interaction between negatively charged laponite and positively charged HRP can strongly affect the heme microenvironment, resulting in the stable signal; it can also lead to a higher available loading of HRP. Moreover, the laponite/Chit composite film can offer a friendly microenvironment for the entrapped enzyme. The applicability of the proposed biosensor as assay of sulfide was tested based on catalytic inhibition principle.

Acknowledgements

The authors are grateful to the financial supports of National Natural Science Foundation of China (Grant no. 20773108, 20905011 and 20810102052), University science research project of Jiangsu Province (09KJB150015), Qing Lan Project of Jiangsu Province, the Natural Science Foundation of Jiangsu (SBK201022537), and the project sponsored for D. Shan by the scientific research foundation for the returned overseas Chinese scholars, State Education Ministry.

References

Bard, A.J., Faulkner, L.R., 2001. Electrochemical Methods Fundamentals and Applications. Wiley, New York.
Chen, H.J., Dong, S.J., 2007. Biosens. Bioelectron. 22, 1811–1815.
Čmelik, J., Machát, J., Otruba, V., Kanicky, V., 2010. Talanta 80, 1777–1781.
Fan, Q., Shan, D., Xue, H.G., He, Y.Y., Cosnier, S., 2007. Biosens. Bioelectron. 22, 816–821.
Freire, R.S., Pessoa, C.A., Mello, L.D., Kubota, L.T., 2003. J. Braz. Chem. Soc. 14, 230–243.
Ghamouss, F., Ledru, S., Ruillé, N., Lantier, F., Boujtita, M., 2006. Anal. Chim. Acta 570, 158–164.
Guenther, E.A., Johnson, K.S., Coale, K.H., 2001. Anal. Chem. 73, 3481–3487.
Harbury, H.A., 1957. J. Biol. Chem. 225, 1009–1024.
Kamin, R.A., Willson, G.S., 1980. Anal. Chem. 52, 1198–1205.
Kolotilina, N.K., Dolgonosov, A.M., 2005. J. Anal. Chem. 60, 738–742.
Kosyakov, A.V., Zavrazhnov, A.Y., Naumov, A.V., 2010. Inorg. Mater. 46, 343–345.
Krajewska, B., 2004. Enzyme Microb. Technol. 35, 126–139.
Krajewska, B., 2005. Sep. Purif. Technol. 41, 305–312.
Laviron, E., 1979. J. Electroanal. Chem. 100, 263–270.
Lawrence, N.S., Davis, J., Compton, R.G., 2000. Talanta 52, 771–784.
Lin, X., Chen, J., Chen, Z., 2000. Electroanalysis 12, 306–310.
Liu, L.H., Zhao, F.Q., Liu, L.Q., Li, J., Zeng, B.Z., 2009. Colloid. Surf. B 68, 93–97.
Ma, H., Hu, N., Rusling, J., 2000. Langmuir 16, 4969–4975.
Mousty, C., Cosnier, S., Shan, D., Mu, S.L., 2001. Anal. Chim. Acta 44, 1–8.
Pecorari, M., Bianco, P., 1998. Electroanalysis 10, 181–186.
Safavi, A., Karimi, M.A., 2002. Talanta 57, 491–500.
Shan, D., Mousty, C., Cosnier, S., Mu, S.L., 2002. J. Electroanal. Chem. 537, 103–109.
Shan, D., Mousty, C., Cosnier, S., Mu, S.L., 2003. Electroanalysis 15, 1506–1512.
Shan, D., Mousty, C., Cosnier, S., 2004a. Anal. Chem. 76, 178–183.
Shan, D., Cosnier, S., Mousty, C., 2004b. Biosens. Bioelectron. 20, 390–396.
Shan, D., Han, E., Xue, H.G., Cosnier, S., 2007. Biomacromolecules 8, 3041–3046.
Shan, D., Wang, Y.N., Xue, H.G., Cosnier, S., Ding, S.N., 2009a. Biosens. Bioelectron. 24, 3555–3561.
Shan, D., Zhang, J., Xue, H.G., Ding, S.N., Cosnier, S., 2009b. Biosens. Bioelectron. 25, 1427–1433.
Shi, Q.F., Li, Q.B., Shan, D., Fan, Q., Xue, H.G., 2008. Mater. Sci. Eng. C 28, 1372–1375.
Tanabe, K., Misona, M., Ono, Y., Hattori, H., 1989. Studies in Surface Science and Catalysis, vol. 51. Elsevier, Amsterdam.
Titova, T.V., Borisova, N.S., Zakharchuk, N.F., 2009. Anal. Chim. Acta 653, 154–160.
Wu, F.H., Xu, J.J., Tian, Y., Hu, Z.C., Wang, L.W., Xian, Y.Z., Jin, L.T., 2008. Biosens. Bioelectron. 24, 198–203.
Xiao, X.L., Luan, Q.F., Yao, X., Zhou, K.B., 2009. Biosens. Bioelectron. 24, 2447–2451.
Xiang, C., Zou, Y., Sun, L., Xu, F., 2009. Sens. Actuators B 136, 158–162.
Xu, X., Liu, S., Ju, H., 2003. Sensors 3, 350–360.
Yamazaki, I., Arisso, T., Hayashi, Y., Yamada, H., Makino, R., 1978. Adv. Biophys. 11, 249–281.
Yan, R., Zhao, F.Q., Li, J.W., Mao, F., Fan, S.S., Zeng, B.Z., 2007. Electrochim. Acta 52, 7425–7431.
Yang, Y.H., Yang, M.H., Wang, H., Jiang, J.H., Shen, G.L., Yu, R.Q., 2004. Sens. Actuators B: Chem. 102, 162–168.
Yin, H.S., Ai, S.Y., Shi, W.J., Zhu, L.S., 2009. Sens. Actuators B: Chem. 137, 747–753.
Zhang, L., Zhang, Q., Lu, X.B., Li, J.H., 2007. Biosens. Bioelectron. 23, 102–106.
Zhao, J.G., Henkens, R.W., Crumbliss, A.L., 1996. Biotechnol. Prog. 12, 703–708.
Zhao, G., Feng, J.J., Xu, J.J., Chen, H.Y., 2005. Electrochem. Commun. 7, 724–729.
Zhao, X.J., Mai, Z.B., Kang, X.H., Zou, X.Y., 2008. Biosens. Bioelectron. 23, 1032–1038.
Zhou, Y.L., Hu, N.F., Zeng, Y.H., Rustling, J.F., 2002. Langmuir 18, 211–219.
Zong, S.Z., Cao, Y., Zhou, Y.M., Ju, H.X., 2006. Langmuir 22, 8915–8919.